Highly Organized Monolayer Arrangement of 2D Materials and Its Applications

Nobuyuki Sakai and Takayoshi Sasaki**

Research Center for Materials Nanoarchitectonics (MANA), National Institute for Materials Science (NIMS), Tsukuba, Ibaraki 305-0044, Japan

Conspectus: 2D materials, also termed 2D nanosheets, have attracted significant interest due to their unique molecularly thin 2D structure to exhibit various attractive properties. They include a diverse range of materials, such as graphene, chalcogenide, oxide, hydroxide, and carbide. Such 2D materials can be produced via the delamination of their precursor layered compounds. Different from graphite and van der Waals layered compounds, there are a wide range of layered materials accommodating interlayer counterions, serving as a trigger for delamination upon exchange with suitable species. Since interlayer galleries swell evenly and infinitely, single-layer nanosheets can be obtained in high yield in the form of a colloidal suspension.

The arrangement of unilamellar 2D nanosheets on a substrate surface, avoiding large gaps and overlaps, is crucial for fully harnessing their performance. A resulting monolayer film of neatly tiled 2D nanosheets can provide a molecularly thin interface and a well-defined crystalline surface, leading to the development of unique properties and reactivities. Consequently, considerable efforts have been focused on developing solution-based assembly techniques, including electrostatic self-assembly, the Langmuir-Blodgett (LB) method, and spin coating, to produce highly organized monolayer films.

In the electrostatic self-assembly process, a substrate with an oppositely charged surface is immersed in the nanosheet suspension, and nanosheets are adsorbed on the substrate through

electrostatic attraction, forming a monolayer film of nanosheets in a self-assembly fashion. In the case of LB and spin coating methods, nanosheets trapped at the air-liquid interface are densely packed in a lateral direction to achieve neat monolayer tiling on a solvent surface, which is then transferred onto a substrate surface. Compared to the electrostatic self-assembled film, the LB method yields a higher-quality monolayer film of nanosheets without large gaps or overlaps thanks to the surface compression. Similar neat tiling has been achieved by using the spin coating method with optimized deposition parameters. The advantage of this method is its ability to fabricate the film in a shorter period (~a few minutes), making it most suitable for practical use.

Neatly tiled monolayer films of nanosheets have been applied to modify the surface and interface properties of materials, as exemplified by the performance enhancement of batteries and epitaxial growth of crystalline thin films. Furthermore, the precise monolayer tiling serves as the fundamental step for constructing multilayer films of each nanosheet or even artificial lattice-like films, where nanosheets are stacked in a designed sequence, allowing for the evolution of sophisticated functionalities via synergetic coupling between constituent nanosheets. It has been demonstrated that heterostructured films, composed of various types of nanosheets, can enhance the individual properties of components and introduce novel functions. The integration of nanosheets with different properties using the methods outlined in this Account will lead to the realization of various next-generation devices.

1. Introduction

Various transition metal oxide nanosheets have been systematically explored since the 1990s.[1–4] With the emergence of graphene, they have gained recognition as an important class of 2D material, leading to extensive research on their synthesis and physical properties.[5–9] Oxide nanosheets based on Ti, Nb, and Ta are wide-gap semiconductors, while those of Mn, Mo, and W exhibit redox ability. Additionally, Ru oxide nanosheets show a high electrical conductivity. In general, oxide nanosheets are characterized by high chemical and thermal stability. These oxide nanosheets find applications in various fields, including dielectrics, magneto-optical materials, and energy conversion/storage devices and are increasingly gaining attention.

The most effective method to obtain nanosheets is through the delamination of precursor layered compounds. Their structure is composed of host layers formed by covalent bonds, which are stacked by relatively weak interactions such as van der Waals force or electrostatic attraction. Consequently, there is a possibility that they can be disintegrated by breaking the weak bonds between the layers. For example, it is well-known that graphite can be mechanically cleaved using adhesive tape in the first report, which is a simple and straightforward method to obtain monolayer graphene, although the yield and reproducibility are low.[10] Furthermore, it has been reported that transition metal dichalcogenides as well as graphite undergo exfoliation into a single layer to several layers upon exposure to ultrasonic waves in an appropriate solvent.[11] Although these two methods are suitably used for studying the physical properties of individual 2D materials, the yield and quality are not satisfactory. The production of monolayer nanosheets with a uniform thickness in high yield is required to construct functional nanostructured materials using nanosheets as building blocks.

Most layered metal oxides accommodate exchangeable interlayer cations. Exchange with suitable guest species can induce a high degree of swelling, ultimately leading to delamination. Soft chemical processes for delaminating a variety of layered hosts have been established,[5–9] and the protocols are described below (Figure 1). When the interlayer is modified with bulky organoammonium ions (e.g., tetrabutylammonium (TBA^+) ion, tetramethylammonium (TMA^+) ion) through ion exchange, a large amount of water is introduced between the layers, causing several to 100 times massive swelling.[12] As a result, the attractive force between the layers significantly weakens, and they fall apart when a shearing force is applied, resulting in charged nanosheets stably dispersed in the solution. Delamination can be understood in terms of infinite swelling. Since all interlayer galleries expand homogeneously, single-layer nanosheets can be obtained at a high yield.[13] The thickness of the nanosheet has a specific value corresponding to the host layer of the parent layered compound, whereas the lateral size of the nanosheet depends on the crystal size of the precursors, the type of organic ammonium ions used for swelling, and the method used to apply shear forces. Using appropriate synthesis conditions, nanosheets with aspect ratios (lateral size/thickness) up to the tens of thousands can be obtained.[14,15]

The controlled arrangement of nanosheets on a substrate to create highly organized single-layer films is a crucial step in designing nanodevices that take advantage of the properties of nanosheets.

While the mechanical transfer process is useful for placing one nanosheet at a specified position on a substrate, it is challenging to regularly arrange many nanosheets over a wide area, making it unsuitable for practical use. On the other hand, solution-based molecular assembly technology can produce highly organized nanostructured films on a large scale and has great potential for practical application. In this Account, we provide an overview of the recent progress in nanosheet tiling using typical assembly technologies (Figure 2), such as electrostatic self-assembly, Langmuir-Blodgett (LB) deposition, and spin coating, along with typical examples of their applications.

2. Neat Monolayer Tiling of Nanosheets

Due to the electrical charge carried by the nanosheets and their dispersion in a solution, they can be assembled into a monolayer film by aligning the nanosheets laterally on a substrate through solution-based processes. These processes include electrostatic self-assembly, LB deposition, and spin coating.

The electrostatic self-assembly method, or sequential adsorption technique, has been employed to assemble nanosheets monodispersed in colloidal suspensions onto various substrates.[16,17] Here, we explain the fabrication procedure using titania nanosheets as a typical example. Initially, a cleaned substrate is precoated with a cationic polymer (polydiallyldimethylammonium ion (PDDA), polyethyleneimine (PEI), etc.) by soaking it in a solution of the polymer. Subsequently, the substrate is immersed in a dispersion of titania nanosheets, and the nanosheets begin to adsorb on the substrate surface via electrostatic attraction. Once the substrate surface is covered with nanosheets and becomes negatively charged,[18] further deposition is inhibited due to repulsion, leading to the formation of a monolayer film through the self-assembly process, as shown by atomic force microscopy (AFM) image (Figure 3A).[19] The height histogram is composed of multiple peaks, the interval of which corresponds to the nanosheet thickness. This indicates that the peaks at 0.0, 1.2, and 2.4 nm represent the regions uncovered, covered by monolayer nanosheets, and covered by overlapped nanosheets, respectively. The relative abundance of each area can be estimated to assess how the nanosheets are adsorbed on the substrate. The area covered with nanosheets is 73%, while the area of uncovered and overlapped regions is 27% and 20%, respectively. In the initial stage of adsorption, the nanosheets are anchored onto the polymer-coated substrate surface, positioning them apart from each other. With prolonged soaking time, a

nanosheet may become adsorbed, even in the gaps between previously adsorbed nanosheets, partially overlapping with adjacent ones. Such partial overlap can occur if the attractive force between a portion of a single nanosheet and the substrate is sufficiently strong to overcome the electrostatic repulsion in the overlapping region. By adjusting the concentration, pH, and immersion time of the nanosheet suspension, the surface coverage with nanosheets can reach approximately 90%, although the area of the overlapped nanosheets also exceeds 40%.[20] Even under such optimized conditions, substantial overlaps and gaps are typically formed. This may be an inevitable consequence of the adsorption of micrometer-sized nanosheets, which is significantly larger than the molecular scale, where self-assembly is effective. One approach to reduce the overlapped area and increase the monolayer region involves using larger nanosheets with a lateral size of several tens of micrometers and subjecting the deposited nanosheets to ultrasonic treatment in an aqueous TBAOH solution. While a portion of the nanosheets that are directly adsorbed on a substrate remains tightly held, overlapped patches are trimmed by ultrasonic cavitation. By reflecting such a film preparation method, the height histogram of the AFM image shows that there are almost no gaps and only a small amount of overlapped regions. Consequently, a high-quality nanosheet film with a monolayer area of 94% and an overlapped area of 6% has been successfully obtained (Figure 3B).[19]

The LB method was originally developed for fabricating organic films by involving the adsorption of amphiphilic molecules at an air-liquid interface and their subsequent transfer to the substrate surface after compression. This technique has proven to be an effective approach for organizing 2D nanosheets, as well. Nanosheets delaminated from aluminosilicate,[21] layered MoS_2,[22] and layered titanate[23] can float by electrostatically linking to amphiphilic organoammonium cations spread at the air-liquid interface. These nanosheets can then be transferred to a substrate surface through the standard LB procedure. Further studies have shown that TBA^+ ions, used as a delaminating agent, exhibit moderate amphiphilic behavior, allowing nanosheets to spontaneously float at the air-liquid interface.[24] The LB process has been successfully applied to various nanosheets without the addition of another surfactant. Initially, the nanosheets are sparsely suspended at the air-liquid interface, and they are gathered and packed laterally by surface compression before being transferred onto a substrate surface. This operation, under optimized conditions, promotes the neat monolayer tiling of nanosheets without large gaps

or overlaps (Figure 3C). The histogram indicates that most area of the film consists of monolayer regions (~97%) with only a few gaps remained, and there is almost no overlap.[25] In comparison to the electrostatic self-assembled film described above, the LB method yields a more ordered and high-quality monolayer film of nanosheets.

Spin coating, widely used in the semiconductor industry for its simplicity and versatility, has also been applied to fabricate films of 2D nanosheets. Nanosheet films ($Ti_{1-\delta}O_2$ and $Ca_2Nb_3O_{10}$), with a thickness ranging from submicrometers to several micrometers, have been obtained by adjusting the concentration of precursor nanosheet suspensions.[26,27] Besides such thick films, it is more crucial to precisely control the film thickness comparable to that of nanosheets, including the formation of a monolayer film of nanosheets. In a pioneering study, a monolayer film of graphene oxide (GO) nanosheets has been successfully fabricated by spin-coating an aqueous GO suspension.[28] By replacing the aqueous phase with organic solvents such as dimethyl sulfoxide (DMSO), monolayer tiling of oxide nanosheets such as $Ti_{0.87}O_2$ and $Ca_2Nb_3O_{10}$ has also been achieved under appropriate spin coating conditions with optimized nanosheet concentration and rotation speed.[29] When the original aqueous suspension is used, the solvent evaporates quickly, leading to rather uncontrollable deposition of nanosheets and extensive overlaps. In contrast, DMSO with suitable viscosity evaporates slowly, providing the necessary time for the nanosheets to align laterally during the spin coating process. Consequently, individual nanosheets are laterally packed with limited gaps, achieving a coverage of approximately 90%, as estimated from the height histogram (Figure 3D).[30] The resulting monolayer film is comparable to that attained by the LB method. This reflects the nanosheet arrangement mechanism by spin coating, as described below. It is noteworthy that the spin coating fabrication procedure is relatively simple, requiring no expert skills, and the process time is much shorter, typically 1 to 2 min, making it suitable for practical use.

Understanding how nanosheets with high 2D anisotropy are deposited into a neatly tiled monolayer film on a substrate by spin coating is of great importance, both scientifically and practically. As schematically illustrated (Figure 4A),[30] during the spin coating, nanosheets are trapped at the air-liquid interface. Their density increases as the thickness of the suspension decreases due to solvent evaporation, ultimately leading to the achievement of neat monolayer tiling of the nanosheets on the liquid surface. As solvent evaporation progresses, the monolayer

film of nanosheets formed on the liquid is transferred to the substrate surface from its center toward the edges. Amphiphilic TBA^+ ions in the suspension play a crucial role in trapping the nanosheets at the air-liquid interface, and the series of processes during spin coating is similar to the monolayer film formation by the LB method.

Nanosheet deposition via spin coating is influenced by various factors, including the size of the substrate, the concentration of the nanosheet suspension, the type of nanosheets, the rotation speed of the spin coating, the ambient temperature, etc. For instance, if the rotation speed is higher than the optimum value, much of the substrate surface is left uncovered (Figure 4B). Conversely, when the rotational speed is lower than the optimum value, significant overlap of nanosheets occurs. Determination of the optimum rotation speed is crucial for achieving neat monolayer tiling of nanosheets across the entire substrate surface. At the beginning of the spin coating process, centrifugal force expels most of the suspension on the substrate, leaving a portion of the liquid that forms a liquid layer several micrometers thick. This thickness is determined by the surface tension between the liquid and the substrate surface and it is found to be proportional to the reciprocal of the square of the rotation speed (ω). Meanwhile, the amount of nanosheets deposited on the substrate surface is proportional to the amount of the remaining dispersion or the thickness of the liquid layer. Therefore, at a rotation speed higher than the optimum value, a relationship is established where the area (A) covered with the nanosheets in a single layer is proportional to the reciprocal of the square of the rotation speed ($A \propto 1/\omega^2$). The intersection of the regression line and the area of the substrate surface provides the optimum rotation speed (ω_{opt}) for achieving neat monolayer tiling of nanosheets across the entire substrate surface (Figure 4C). This relationship remains valid even when the size of the substrate, the concentration of the nanosheet suspension, and the type of nanosheet are changed, making it a useful and convenient method for predicting the optimum rotation speed for each film fabrication via spin coating.[30]

3. Applications of Neatly Tiled Monolayer Films of Nanosheets

The introduction of a monolayer film of nanosheets enables the control of surface and interface properties of materials, with the expectation of enhancing physicochemical properties and developing novel functions.

3.1. Ultrathin Solid Electrolyte That Lowers Interfacial Resistance in All-Solid-State Battery

Tantalum oxide (TaO_3) nanosheets serve as free-standing solid electrolytes with an ultimate thickness of 1 nm.[31] When the surface of the $LiCoO_2$ cathode is spin-coated with a monolayer film of TaO_3 nanosheets, the interfacial resistance between the cathode and the sulfide-based solid electrolyte (thio-LISICON) is reduced by 2 orders of magnitude (Figure 5A). The TaO_3 nanosheet is electrically insulating and possesses a unique 2D mesh structure with open channels approximately the same size as lithium ions. These features inhibit electron conduction at the interface while allowing lithium ions to pass through, bringing about a drastic reduction in interfacial resistance. This remarkable behavior holds promise for practical applications in all-solid-state lithium-ion batteries.

3.2. Reversible Zinc Electrode Coated with Nanosheets

Zn-based energy storage is gaining attention due to its low cost, high energy density, high safety, and environmentally friendly manufacturing process. However, it faces challenges such as dendrite growth due to uneven plating/stripping of Zn and side reactions, including hydrogen gas generation. When a monolayer film of $Ti_{0.87}O_2$ nanosheets is deposited on the Zn electrode surface by spin coating, dendrite growth is substantially suppressed, achieving a reversible Zn electrode (Figure 5B).[32] This is attributed to the negatively charged nanosheets attracting Zn^{2+} ions near the electrode with a high density and uniform distribution. As a result, the overpotential for Zn nucleation is significantly reduced and H_2 generation is suppressed, leading to uniform Zn precipitation without the formation of dendrites. Additionally, the ultrathin interface of the nanosheets maintains the conductivity and specific capacity of the Zn electrode. The lifetime of charge/discharge cycles involving plating/stripping of the Zn electrode has been improved by more than 13 times. This outcome establishes an economical and efficient strategy for molecular-scale interface engineering that enables the practical application of Zn electrodes. Furthermore, this approach is expected to be applied to other metal electrodes such as Li, Na, Al, and Mg.

3.3. Microepitaxial Growth Using Nanosheets as a Seed Layer

Epitaxial growth of crystalline thin films is extensively used in the manufacturing of modern devices. However, there are significant challenges related to lattice matching between the substrate and the growing crystalline layer, often requiring the use of expensive single-crystal substrates. Nanosheets, being 2D single crystals with atomically flat surfaces, can serve as 1-nm-thick seed layers, promoting oriented crystal growth on cost-effective substrates such as glass after covered with nanosheets (Figure 5C).[33] Here, it should be pointed out that heteroepitaxial growth is promoted in the domain of the nanosheet size. Thus, the unidirectional growth is attained when viewed across the substrate because each nanosheet is randomly aligned in the lateral azimuth direction. By employing $Ca_2Nb_3O_{10}$ nanosheets with a 2D square lattice, oriented crystal films of cubic $SrTiO_3$ and tetragonal anatase TiO_2 can be grown. Similarly, an oriented film of wurtzite-type ZnO crystal can be grown on MnO_2 nanosheets with a 2D hexagonal structure. Furthermore, as an interesting and versatile example, the oriented growth of $SrTiO_3$ films along various crystallographic axes has been demonstrated by selecting nanosheets with appropriate 2D structures (Figure 5D).[34] When $Ca_2Nb_3O_{10}$ nanosheets are used as seed layers, oriented growth along the [100] direction is promoted. Conversely, when $Ti_{0.87}O_2$ nanosheets with a 2D rectangular lattice and MoO_2 nanosheets with a 2D pseudohexagonal lattice are used, preferential growth along the [110] and [111] directions is achieved, respectively. Moreover, the nanosheet-based seed layer can be introduced on various substrates, including plastic, where oriented ZnO crystal films are grown at room temperature.[35]

3.4. Scission of Nanosheets via Adsorption onto Nonflat Substrate Surfaces

Recently, it has been observed that when $Ti_{0.87}O_2$ nanosheets are deposited by spin coating on a substrate with a rough surface, cracks running orthogonally are generated inside the nanosheets, eventually sectioning them into rectangular shapes (Figure 5E).[36] When the nanosheets, floating on the solvent surface, begin to adsorb to the substrate surface due to solvent evaporation during the spin coating process, one nanosheet simultaneously contacts multiple convex points on the substrate surface and tends to follow the shape of the substrate at each location. As the area of the nanosheet is smaller than the actual area of the nonflat substrate surface, tensile stress is generated in the lateral direction of the nanosheet during the adsorption progress. The 2D anisotropy of the nanosheets is a key factor in breaking chemical bonds (~670 kJ/mol) by tensile stress based on intermolecular forces (~5 kJ/mol). When the anisotropy of the nanosheets is large enough, the

integrated tensile stress along the nanosheet surface, caused by adhesion energy due to the intermolecular forces, can exceed the energy required to cleave the bonds in the nanosheets, resulting in the spontaneous sectioning of the nanosheets along the fundamental crystallographic axes ([01] and [10]; Figure 5F). This phenomenon is observed for all nanosheets on a substrate of several square centimeters, leading to the simultaneous sectioning of millions of nanosheets. This interesting discovery may introduce a new processing technique for cutting and shaping various 2D materials. Furthermore, the cut surface at the edges of the nanosheets, as well as the gaps across the cracks, may prove useful as a reaction field to modify the properties of the nanosheets, since the edges of the nanosheet generally show high reactivities.[37]

4. Construction of Multilayered or Heterostructured Films of Nanosheets

The monolayer deposition can be repeated layer-by-layer to form a multilayer film, and the regular film growth can be verified using various techniques, such as UV-vis absorption spectroscopy and X-ray diffraction (XRD). For instance, the formation of a monolayer film of titania nanosheets results in an increase in absorbance in the UV region, and the absorbance linearly enhances with the number of nanosheet adsorption cycles via electrostatic self-assembly using PDDA as a countercation (Figure 6A).[20] This suggests that a film of nanosheets equivalent to the first monolayer is formed in each adsorption cycle. Furthermore, the multilayer films formed in this way exhibit Bragg diffraction peaks in the low-angle region of the XRD pattern, indicating that the nanosheets are stacked regularly at intervals of 1.4-1.5 nm, corresponding to the sum of the thickness of titania nanosheets and PDDA layers. Multilayer films of nanosheets can also be constructed by repeating the LB transfer or spin coating. In these processes, more highly ordered multilayer films can be obtained by using nanosheets with larger lateral sizes, such as titania nanosheets with a lateral size of several tens of micrometers.[25,29] There is no essential difference in the surface morphology observed by AFM between a monolayer film and a multilayer film, suggesting that a tiled nanosheet film arranged on a liquid surface is transferred in each cycle. Transmission electron microscopy (TEM) observation of a cross-section of the multilayer film shows regularly stacked fringes corresponding to the layer-by-layer assembled nanosheets (Figure 6B). The XRD pattern for the multilayer film yields sharp basal diffraction peaks up to the seventh order (Figure 6C). Analysis of their profile suggests the entire thickness of the multilayer film is coherent to X-rays, indicating that the lattice distortion is negligibly small. Furthermore, the basal

peaks are accompanied by small satellite ripples arising from the Laue interference functions. This high film quality is comparable to or even higher than artificial lattices constructed by modern vapor deposition processes, and a nearly perfect interface between the nanosheets in the stacking direction can be created at room temperature.

More importantly, it is possible to construct heterostructured or superlattice-like films in which different nanosheets are assembled in a designed order, potentially leading to synergistic enhancements of individual properties and the development of novel functions. For instance, titania nanosheets are semiconducting, while MnO_2 nanosheets are redox-active. These two types of nanosheets can be electrostatically assembled in various designed sequences, with a polymer layer intervening as an electrostatic glue (Figure 6D). In the fabricated superlattice-like films, excited electrons of titania nanosheets under UV light are injected into the MnO_2 nanosheets, indicating photochemical energy storage.[38] A heterostructured film consisting of a monolayer film of titania nanosheets on top of reduced graphene oxide shows superior properties of photoinduced wettability conversion based on the efficient separation of photogenerated carriers at the large interface between the two types of nanosheets (Figure 6E).[39] A superlattice-like film constructed by the LB method exhibits novel properties based on new electronic states generated at the nearly perfect interface. For example, while two different types of nanosheets with perovskite structures ($LaNb_2O_7$ and $Ca_2Nb_3O_{10}$) are both paraelectric, a superlattice-like structure using these nanosheets as constituent elements exhibits ferroelectricity.[40] Multiferroic materials can also be constructed through rational design. A high-quality superlattice-like film made of alternating layers of dielectric $Ca_2Nb_3O_{10}$ nanosheets and ferromagnetic $Ti_{0.8}Co_{0.2}O_2$ nanosheets induces ferroelectricity at room temperature in the presence of ferromagnetic order due to the heterostructure with strong magnetoelectric coupling (Figure 6F).[41] Such a superlattice-like material is structurally unique, and it is not realistic to synthesize it in bulk by a conventional solid-state calcination process. Layer-by-layer engineering of nanosheets provides a new route to realize artificial nanoarchitecture with advanced functionalities. Interestingly, when a mixed suspension containing $Ti_{0.87}O_2$ and $Ca_2Nb_3O_{10}$ nanosheets is employed for spin coating, a unique monolayer film, in which the two types of nanosheets are laterally packed in a mosaic pattern, can be created (Figure 6G).[42] Due to the diverse and attractive functions exhibited by nanosheets, it is anticipated that hierarchical

nanostructures, incorporating both vertical and horizontal assembly of heterostructures, will provide a powerful route in the design of next-generation functional materials.

5. Summary and Outlook

In this Account, we explore the arrangement of nanosheets dispersed in a colloidal suspension into neatly tiled monolayer films on a substrate based on various solution processes, including electrostatic self-assembly, the LB method, and spin coating. Introducing a monolayer film of nanosheets onto a substrate allows for the control of surface and interface properties, enhancing physicochemical characteristics and fostering novel functions. Moreover, through the repeated deposition of monolayers in a designed sequence, it becomes possible to construct multilayer and superlattice-like films via artificial lattice engineering, offering the potential for enhanced and sophisticated functionalities. Recently, innovative techniques such as single droplet assembly[43] have been developed for monolayer tiling, and the automation of the assembly process using robots has been demonstrated,[44] anticipating applications for industrialization.

The nanosheet library continues to expand with the development of new layered compounds and exfoliation methods. Integrating nanosheets with various properties through the molecular assembly approaches described in this article holds great potential to realize advanced functions crucial for next-generation electronic, optical, and energy storage applications. The solution-based assembly technology presented here is not limited to oxide nanosheets but is also applicable to various charged nanosheets including chalcogenides, carbides, hydroxides, and more. To further enhance their functionality, it is crucial not only to control the size and shape of each nanosheet but also to assemble them on a substrate while controlling their crystallographic orientation, leading to a pseudosingle-crystal film of regularly aligned nanosheets. One ambitious idea is to synthesize nanosheets with uniform size and shape through advanced exfoliation and processing technologies. Deposition of such nanosheets holds the promise of achieving their ultimate tiling via self-assembly principles. Though this strategy poses challenges, it is worth exploring for the further development of 2D materials.

Corresponding Authors

* **Nobuyuki Sakai** – Research Center for Materials Nanoarchitectonics (MANA), National Institute for Materials Science (NIMS), Tsukuba, Ibaraki 305-0044, Japan; ORCID: 0000-0002-9395-6751; E-mail: sakai.nobuyuki@nims.go.jp

* **Takayoshi Sasaki** – Research Center for Materials Nanoarchitectonics (MANA), National Institute for Materials Science (NIMS), Tsukuba, Ibaraki 305-0044, Japan; ORCID: 0000-0002-2872-0427; E-mail: sasaki.takayoshi@nims.go.jp

Author Contributions

The manuscript was written through contributions of all authors.

Notes

The authors declare no competing financial interest.

Biographies

Nobuyuki Sakai is a Principal Researcher at Research Center for Materials Nanoarchitectonics (MANA) at National Institute for Materials Science (NIMS) in Japan. He received his Ph.D. in Engineering from the University of Tokyo in 2002 and then worked as a postdoctoral researcher at NIMS. He was appointed as an Assistant Professor at the University of Tokyo in 2006 and he joined NIMS as a staff member in 2013. His current research interests are in the synthesis and assembly of 2D oxide nanosheets and their applications in energy conversion and storage.

Takayoshi Sasaki is a Fellow at National Institute for Materials Science (NIMS). He received his Ph.D. in Chemistry from the University of Tokyo in 1985. Since 1980, he has been working for the National Institute for Research in Inorganic Materials (NIRIM), Japan, which was reorganized into NIMS in 2001. His current interest has focused on 2D oxide and hydroxide nanosheets obtained by delaminating layered materials.

Acknowledgment

MANA is supported by World Premier International Research Center Initiative (WPI), MEXT, Japan. This work was supported by JST, CREST Grant Number JPMJCR22B1, Japan.

References

(1) Treacy, M. M. J.; Rice, S. B.; Jacobson, A. J.; Lewandowski, J. T. Electron Microscopy Study of Delamination in Dispersions of the Perovskite-Related Layered Phases $K[Ca_2Na_{n-3}Nb_nO_{3n+1}]$: Evidence for Single-Layer Formation. *Chem. Mater.* **1990**, *2*, 279–286.

(2) Sasaki, T.; Watanabe, M.; Hashizume, H.; Yamada, H.; Nakazawa, H. Macromolecule-like Aspects for a Colloidal Suspension of an Exfoliated Titanate. Pairwise Association of Nanosheets and Dynamic Reassembling Process Initiated from It. *J. Am. Chem. Soc.* **1996**, *118*, 8329–8335.

(3) Sasaki, T.; Watanabe, M. Osmotic Swelling to Exfoliation. Exceptionally High Degrees of Hydration of a Layered Titanate. *J. Am. Chem. Soc.* **1998**, *120*, 4682–4689.

(4) Schaak, R. E.; Mallouk, T. E. Perovskites by Design: A Toolbox of Solid-State Reactions. *Chem. Mater.* **2002**, *14*, 1455–1471.

(5) Ma, R.; Sasaki, T. Nanosheets of Oxides and Hydroxides: Ultimate 2D Charge-Bearing Functional Crystallites. *Adv. Mater.* **2010**, *22*, 5082–5104.

(6) ten Elshof, J. E.; Yuan, H.; Gonzalez Rodriguez, P. Two-Dimensional Metal Oxide and Metal Hydroxide Nanosheets: Synthesis, Controlled Assembly and Applications in Energy Conversion and Storage. *Adv. Energy Mater.* **2016**, *6*, 1600355.

(7) Uppuluri, R.; Sen Gupta, A.; Rosas, A. S.; Mallouk, T. E. Soft Chemistry of Ion-Exchangeable Layered Metal Oxides. *Chem. Soc. Rev.* **2018**, *47*, 2401–2430.

(8) Dudko, V.; Khoruzhenko, O.; Weiß, S.; Daab, M.; Loch, P.; Schwieger, W.; Breu, J. Repulsive Osmotic Delamination: 1D Dissolution of 2D Materials. *Adv. Mater. Technol.* **2023**, *8*, 2200553.

(9) Liu, T.; Miao, L.; Yao, F.; Zhang, W.; Zhao, W.; Yang, D.; Feng, Q.; Hu, D. Structure, Properties, Preparation, and Application of Layered Titanates. *Inorg. Chem.* **2024**, *63*, 1–26.

(10) Novoselov, K. S.; Geim, A. K.; Morozov, S. V.; Jiang, D.; Zhang, Y.; Dubonos, S. V.; Grigorieva, I. V.; Firsov, A. A. Electric Field Effect in Atomically Thin Carbon Films. *Science* **2004**, *306*, 666–669.

(11) Coleman, J. N.; Lotya, M.; O'Neill, A.; Bergin, S. D.; King, P. J.; Khan, U.; Young, K.; Gaucher, A.; De, S.; Smith, R. J.; Shvets, I. V.; Arora, S. K.; Stanton, G.; Kim, H.-Y.; Lee, K.; Kim, G. T.; Duesberg, G. S.; Hallam, T.; Boland, J. J.; Wang, J. J.; Donegan, J. F.; Grunlan, J. C.; Moriarty, G.; Shmeliov, A.; Nicholls, R. J.; Perkins, J. M.; Grieveson, E. M.; Theuwissen, K.; McComb, D. W.; Nellist, P. D.; Nicolosi, V. Two-Dimensional Nanosheets Produced by Liquid Exfoliation of Layered Materials. *Science* **2011**, *331*, 568–571.

(12) Geng, F.; Ma, R.; Nakamura, A.; Akatsuka, K.; Ebina, Y.; Yamauchi, Y.; Miyamoto, N.; Tateyama, Y.; Sasaki, T. Unusually Stable ~100-Fold Reversible and Instantaneous Swelling of Inorganic Layered Materials. *Nat. Commun.* **2013**, *4*, 1632.

(13) Wang, L.; Sasaki, T. Titanium Oxide Nanosheets: Graphene Analogues with Versatile Functionalities. *Chem. Rev.* **2014**, *114*, 9455–9486.

(14) Tanaka, T.; Ebina, Y.; Takada, K.; Kurashima, K.; Sasaki, T. Oversized Titania Nanosheet Crystallites Derived from Flux-Grown Layered Titanate Single Crystals. *Chem. Mater.* **2003**, *15*, 3564–3568.

(15) Maluangnont, T.; Matsuba, K.; Geng, F.; Ma, R.; Yamauchi, Y.; Sasaki, T. Osmotic Swelling of Layered Compounds as a Route to Producing High-Quality Two-Dimensional Materials. A Comparative Study of Tetramethylammonium versus Tetrabutylammonium Cation in a Lepidocrocite-Type Titanate. *Chem. Mater.* **2013**, *25*, 3137–3146.

(16) Kleinfeld, E. R.; Ferguson, G. S. Stepwise Formation of Multilayered Nanostructural Films from Macromolecular Precursors. *Science* **1994**, *265*, 370–373.

(17) Keller, S. W.; Kim, H.-N.; Mallouk, T. E. Layer-by-Layer Assembly of Intercalation Compounds and Heterostructures on Surfaces: Toward Molecular "Beaker" Epitaxy. *J. Am. Chem. Soc.* **1994**, *116*, 8817–8818.

(18) Decher, G. Fuzzy Nanoassemblies: Toward Layered Polymeric Multicomposites. *Science* **1997**, *277*, 1232–1237.

(19) Tanaka, T.; Fukuda, K.; Ebina, Y.; Takada, K.; Sasaki, T. Highly Organized Self-Assembled Monolayer and Multilayer Films of Titania Nanosheets. *Adv. Mater.* **2004**, *16*, 872–875.

(20) Sasaki, T.; Ebina, Y.; Tanaka, T.; Harada, M.; Watanabe, M.; Decher, G. Layer-by-Layer Assembly of Titania Nanosheet/Polycation Composite Films. *Chem. Mater.* **2001**, *13*, 4661–4667.

(21) Inukai, K.; Hotta, Y.; Taniguchi, M.; Tomura, S.; Yamagishi, A. Formation of a Clay Monolayer at an Air–Water Interface. *J. Chem. Soc., Chem. Commun.* **1994**, 959.

(22) Taguchi, Y.; Kimura, R.; Azumi, R.; Tachibana, H.; Koshizaki, N.; Shimomura, M.; Momozawa, N.; Sakai, H.; Abe, M.; Matsumoto, M. Fabrication of Hybrid Layered Films of MoS_2 and an Amphiphilic Ammonium Cation Using the Langmuir–Blodgett Technique. *Langmuir* **1998**, *14*, 6550–6555.

(23) Yamaki, T.; Asai, K. Alternate Multilayer Deposition from Ammonium Amphiphiles and Titanium Dioxide Crystalline Nanosheets Using the Langmuir–Blodgett Technique. *Langmuir* **2001**, *17*, 2564–2567.

(24) Muramatsu, M.; Akatsuka, K.; Ebina, Y.; Wang, K.; Sasaki, T.; Ishida, T.; Miyake, K.; Haga, M. Fabrication of Densely Packed Titania Nanosheet Films on Solid Surface by Use of Langmuir–Blodgett Deposition Method without Amphiphilic Additives. *Langmuir* **2005**, *21*, 6590–6595.

(25) Akatsuka, K.; Haga, M.; Ebina, Y.; Osada, M.; Fukuda, K.; Sasaki, T. Construction of Highly Ordered Lamellar Nanostructures through Langmuir–Blodgett Deposition of Molecularly Thin Titania Nanosheets Tens of Micrometers Wide and Their Excellent Dielectric Properties. *ACS Nano* **2009**, *3*, 1097–1106.

(26) Abe, R.; Shinohara, K.; Tanaka, A.; Hara, M.; Kondo, J. N.; Domen, K. Preparation of Thin Films of a Layered Titanate by the Exfoliation of $Cs_xTi_{(2-x/4)}\square_{x/4}O_4$. *Chem. Mater.* **1998**, *10*, 329–333.

(27) Ganter, P.; Lotsch, B. V. Photocatalytic Nanosheet Lithography: Photolithography based on Organically Modified Photoactive 2D Nanosheets. *Angew. Chem. Int. Ed.* **2017**, *56*, 8389–8392.

(28) Kim, J. W.; Kang, D.; Kim, T. H.; Lee, S. G.; Byun, N.; Lee, D. W.; Seo, B. H.; Ruoff, R. S.; Shin, H. S. Mosaic-like Monolayer of Graphene Oxide Sheets Decorated with Tetrabutylammonium Ions. *ACS Nano* **2013**, *7*, 8082–8088.

(29) Matsuba, K.; Wang, C.; Saruwatari, K.; Uesusuki, Y.; Akatsuka, K.; Osada, M.; Ebina, Y.; Ma, R.; Sasaki, T. Neat Monolayer Tiling of Molecularly Thin Two-Dimensional Materials in 1 min. *Sci. Adv.* **2017**, *3*, e1700414.

(30) Sakai, N.; Sasaki, T. Guidelines for Arranging 2D Nanosheets into Neatly Tiled Monolayer Films by a Spin-Coating Process. *Langmuir* **2022**, *38*, 12399–12407.

(31) Xu, X.; Takada, K.; Fukuda, K.; Ohnishi, T.; Akatsuka, K.; Osada, M.; Hang, B. T.; Kumagai, K.; Sekiguchi, T.; Sasaki, T. Tantalum Oxide Nanomesh as Self-Standing One Nanometre Thick Electrolyte. *Energy Environ. Sci.* **2011**, *4*, 3509–3512.

(32) Wang, C.; Sakai, N.; Ebina, Y.; Tang, D.; Ma, R.; Sasaki, T. One-Nanometer-Thick Interfaces of Titania Nanosheets for Reversible Zn-Metal Electrodes. *ACS Mater. Lett.* **2023**, *5*, 2156–2163.

(33) Shibata, T.; Fukuda, K.; Ebina, Y.; Kogure, T.; Sasaki, T. One-Nanometer-Thick Seed Layer of Unilamellar Nanosheets Promotes Oriented Growth of Oxide Crystal Films. *Adv. Mater.* **2008**, *20*, 231–235.

(34) Shibata, T.; Takano, H.; Ebina, Y.; Kim, D. S.; Ozawa, T. C.; Akatsuka, K.; Ohnishi, T.; Takada, K.; Kogure, T.; Sasaki, T. Versatile van der Waals Epitaxy-like Growth of Crystal

Films Using Two-Dimensional Nanosheets as a Seed Layer: Orientation Tuning of $SrTiO_3$ Films along Three Important Axes on Glass Substrates. *J. Mater. Chem. C* **2014**, *2*, 441–449.

(35) Shibata, T.; Ohnishi, T.; Sakaguchi, I.; Osada, M.; Takada, K.; Kogure, T.; Sasaki, T. Well-Controlled Crystal Growth of Zinc Oxide Films on Plastics at Room Temperature Using 2D Nanosheet Seed Layer. *J. Phys. Chem. C* **2009**, *113*, 19096–19101.

(36) Sakai, N.; Suzuki, M.; Sasaki, T. Scission of 2D Inorganic Nanosheets via Physical Adsorption on a Nonflat Surface. *Adv. Mater. Interfaces* **2022**, *9*, 2102591.

(37) Kaschak, D. M.; Johnson, S. A.; Hooks, D. E.; Kim, H.-N.; Ward, M. D.; Mallouk, T. E. Chemistry on the Edge: A Microscopic Analysis of the Intercalation, Exfoliation, Edge Functionalization, and Monolayer Surface Tiling Reactions of α-Zirconium Phosphate. *J. Am. Chem. Soc.* **1998**, *120*, 10887–10894.

(38) Sakai, N.; Fukuda, K.; Omomo, Y.; Ebina, Y.; Takada, K.; Sasaki, T. Hetero-Nanostructured Films of Titanium and Manganese Oxide Nanosheets: Photoinduced Charge Transfer and Electrochemical Properties. *J. Phys. Chem. C* **2008**, *112*, 5197–5202.

(39) Sakai, N.; Kamanaka, K.; Sasaki, T. Modulation of Photochemical Activity of Titania Nanosheets via Heteroassembly with Reduced Graphene Oxide. Enhancement of Photoinduced Hydrophilic Conversion Properties. *J. Phys. Chem. C* **2016**, *120*, 23944–23950.

(40) Li, B.-W.; Osada, M.; Ozawa, T. C.; Ebina, Y.; Akatsuka, K.; Ma, R.; Funakubo, H.; Sasaki, T. Engineered Interfaces of Artificial Perovskite Oxide Superlattices via Nanosheet Deposition Process. *ACS Nano* **2010**, *4*, 6673–6680.

(41) Li, B.-W.; Osada, M.; Ebina, Y.; Ueda, S.; Sasaki, T. Coexistence of Magnetic Order and Ferroelectricity at 2D Nanosheet Interfaces. *J. Am. Chem. Soc.* **2016**, *138*, 7621–7625.

(42) Yano, H.; Sakai, N.; Ebina, Y.; Ma, R.; Osada, M.; Fujimoto, K.; Sasaki, T. Construction of Multilayer Films and Superlattice- and Mosaic-like Heterostructures of 2D Metal Oxide Nanosheets via a Facile Spin-coating Process. *ACS Appl. Mater. Interfaces* **2021**, *13*, 43258–43265.

(43) Shi, Y.; Osada, M.; Ebina, Y.; Sasaki, T. Single Droplet Assembly for Two-Dimensional Nanosheet Tiling. *ACS Nano* **2020**, *14*, 15216–15226.

(44) Shi, Y.; Yamamoto, E.; Kobayashi, M.; Osada, M. Automated One-Drop Assembly for Facile 2D Film Deposition. *ACS Appl. Mater. Interfaces* **2023**, *15*, 22737–22743.

Figures

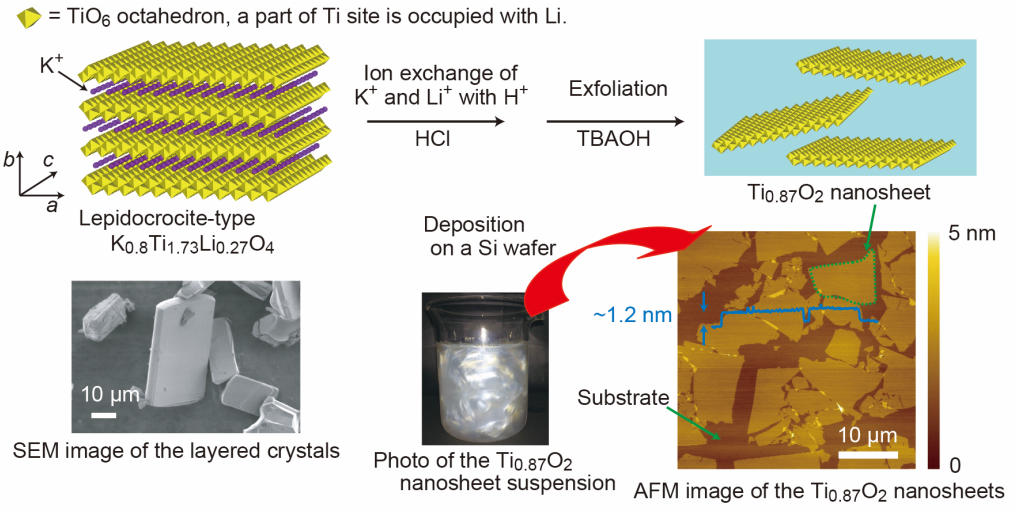

Figure 1. Schematic illustration depicting the delamination process of the layered titanate into titania nanosheets. These nanosheets are acquired as a colloidal suspension, and a uniform thickness of 1.2 nm is observed.

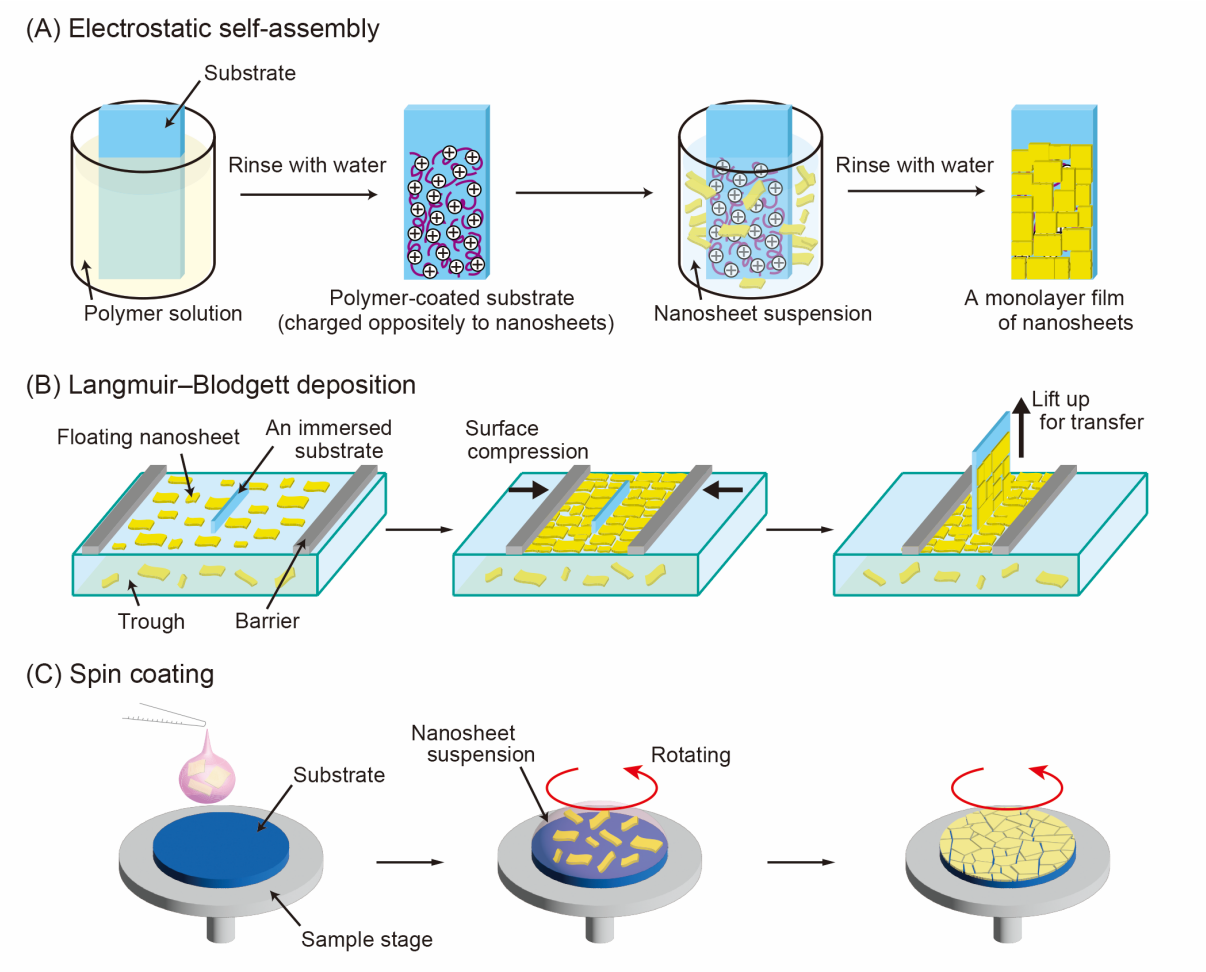

Figure 2. Solution-based assembly techniques, such as (A) electrostatic self-assembly, (B) Langmuir–Blodgett deposition, and (C) spin coating, for the production of highly organized monolayer films of nanosheets.

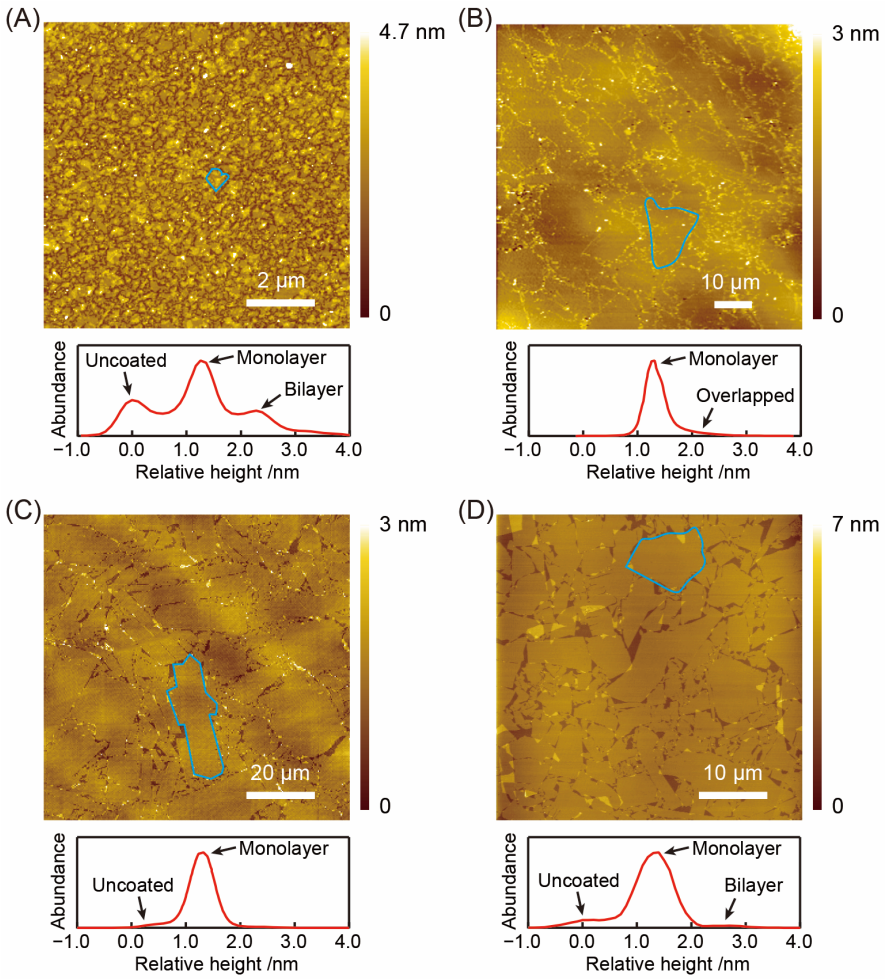

Figure 3. AFM images showing (A) a monolayer film of submicrometer-sized titania nanosheets prepared through electrostatic self-assembly,[19] (B) monolayer films of oversized titania nanosheets obtained via electrostatic self-assembly followed by ultrasonic treatment,[19] (C) LB method,[25] and (D) spin coating. For clarity, a selected nanosheet is outlined in each image. Height histogram for each AFM image is also displayed. Reprinted with permission from ref 19. Copyright 2004 Wiley-VCH Verlag GmbH and Co. KGaA, Weinheim. Reproduced from ref 25. Copyright 2009 American Chemical Society.

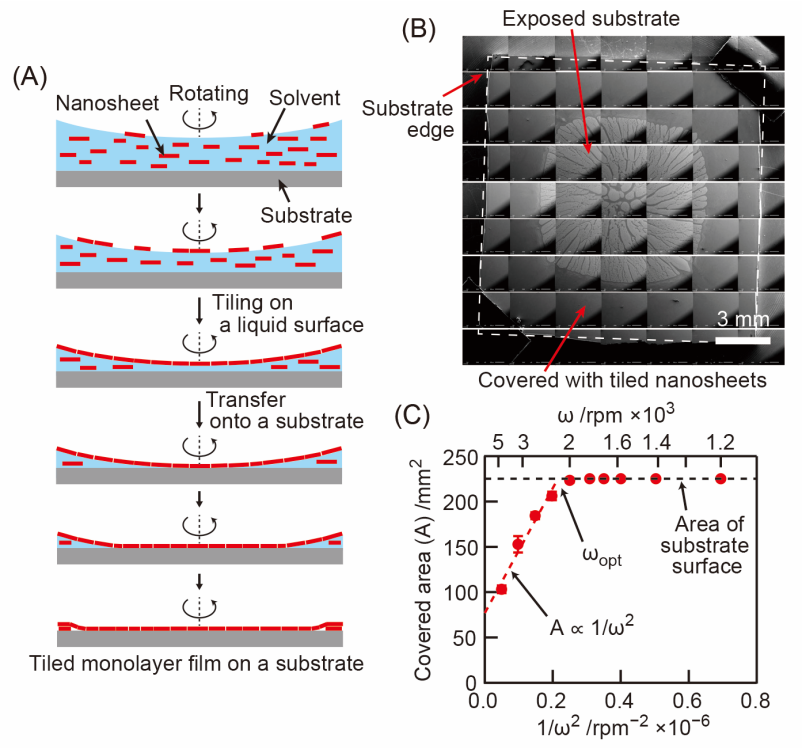

Figure 4. (A) Schematic illustration of the monolayer film formation process using spin coating method on a substrate. (B) Assembly of SEM images of $Ti_{0.87}O_2$ nanosheets on an ITO substrate spin-coated at 3200 rpm. (C) Area of the covered region plotted against $1/\omega^2$ to estimate the optimum rotation speed (ω_{opt}) during spin coating of $Ti_{0.87}O_2$ nanosheet suspension (0.1 wt %) on a 15 mm × 15 mm substrate. Reproduced from ref 30. Copyright 2022 American Chemical Society.

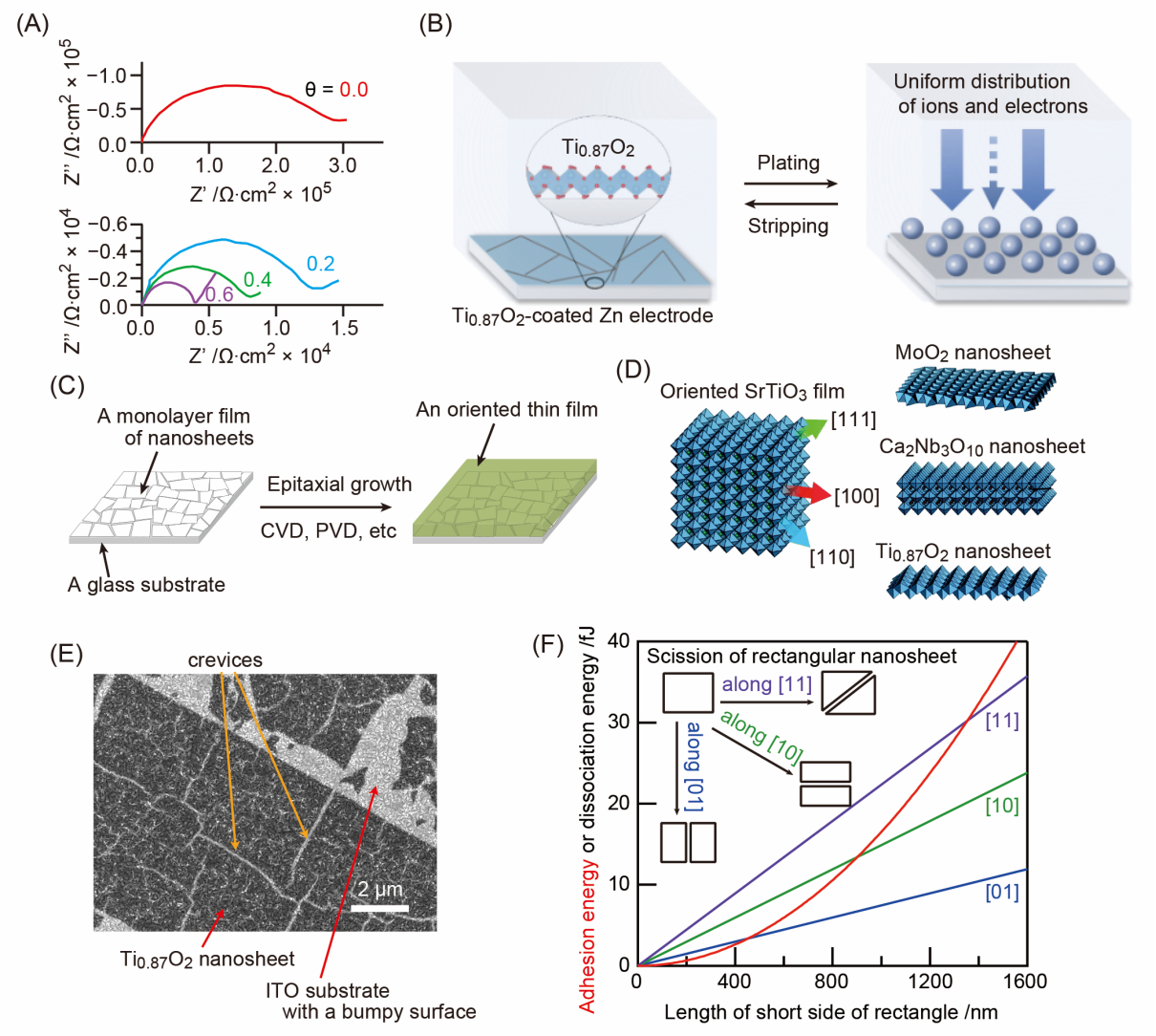

Figure 5. (A) Impedance of $LiCoO_2$ electrodes with varying TaO_3 nanosheet coverage (θ). Reproduced from ref 31. Copyright 2011 The Royal Society of Chemistry. (B) Reversible plating/stripping of Zn on zinc electrodes coated with $Ti_{0.87}O_2$ nanosheets. Reproduced from ref 32. Copyright 2023 American Chemical Society. (C) Schematic explanation of oriented thin film growth on a nanosheet seed layer. (D) Schematic illustration of $Ca_2Nb_3O_{10}$, $Ti_{0.87}O_2$, and MoO_2 nanosheet structures and corresponding $SrTiO_3$ crystal planes. Reprinted with permission from ref 34. Copyright 2014 The Royal Society of Chemistry. (E) SEM image of $Ti_{0.87}O_2$ nanosheets spin-coated on a bumpy ITO substrate surface. (F) Adhesion energy upon $Ti_{0.87}O_2$ nanosheet adsorption on ITO surface (red) and total dissociation energy of Ti–O bonds plotted against nanosheet size, cleaved along [01] (blue), [10] (green), and [11] (purple) axes. Reprinted with permission from ref 36. Copyright 2022 Wiley-VCH GmbH.

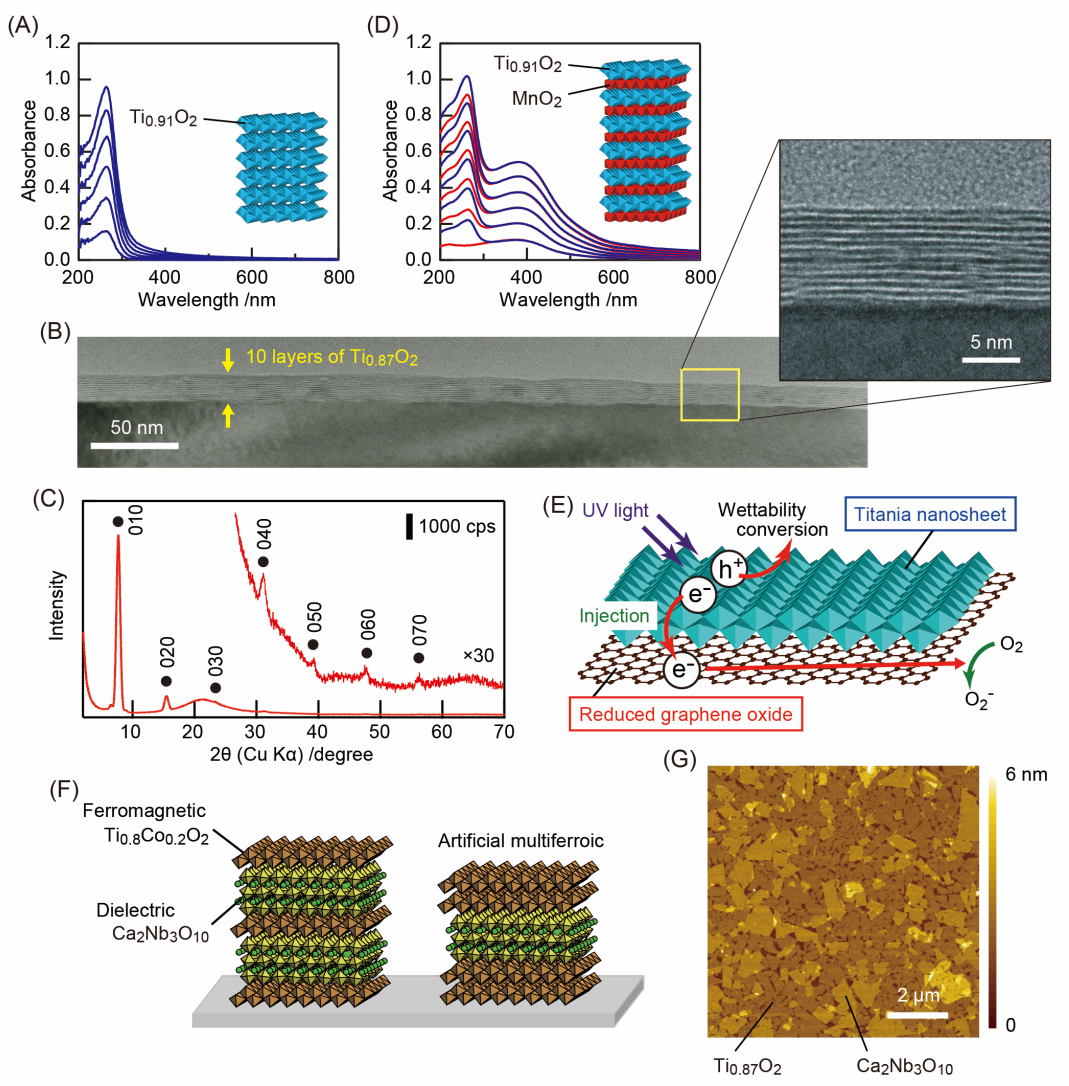

Figure 6. (A) UV–vis absorption spectra of $Ti_{0.91}O_2$ nanosheet multilayer films. (B) Cross-sectional TEM image and (C) XRD pattern of a 10-layer film of $Ti_{0.87}O_2$ nanosheets. Reproduced from ref 25. Copyright 2009 American Chemical Society. (D) UV–vis absorption spectra of heterostructured films with alternately stacked $Ti_{0.91}O_2$ and MnO_2 nanosheets. Reproduced from ref 38. Copyright 2008 American Chemical Society. (E) Schematic illustration of efficient charge separation with a titania nanosheet stacked on reduced graphene oxide. Reproduced from ref 39. Copyright 2016 American Chemical Society. (F) Schematic of a superlattice-like structure, combining $Ti_{0.8}Co_{0.2}O_2$ and $Ca_2Nb_3O_{10}$ nanosheets, creating artificial multiferroic materials. Reproduced from ref 41. Copyright 2016 American Chemical Society. (G) AFM image of a mixed monolayer film of $Ca_2Nb_3O_{10}$ and $Ti_{0.87}O_2$ nanosheets spin-coated on a Si substrate. Reproduced from ref 42. Copyright 2021 American Chemical Society.